Electrochimica Acta 270 (2018) 264–273

Contents lists available at ScienceDirect

Electrochimica Acta

journal homepage: www.elsevier.com/locate/electacta

3-D inkjet-printed solid oxide electrochemical reactors. II. LSM - YSZ electrodes

N.M. Farandos, T. Li, G.H. Kelsall*

Department of Chemical Engineering, Imperial College London, London SW7 2AZ, UK

ARTICLE INFO

Article history:
Received 2 January 2018
Received in revised form
11 March 2018
Accepted 15 March 2018
Available online 16 March 2018

Keywords:
Inkjet printing
Reversible solid oxide fuel cell - electrolyser
Yttria-stabilised zirconia (YSZ)
Lanthanum strontium manganite (LSM)
CO_2 electrolysis

ABSTRACT

Inkjet printing is an economical additive manufacturing technique with minimal material waste, which offers a high degree of control over vertical resolution, so lending itself well to the fabrication of the functional layers of solid oxide electrochemical reactors. We formulated a printable and stable colloidal dispersion of $La_{0.8}Sr_{0.2}MnO_3$ (LSM) - $(Y_2O_3)_{0.08}(ZrO_2)_{0.92}$ (YSZ) ink to print sequentially onto an inkjet-printed YSZ electrolyte sintered to a Ni-YSZ substrate to form the cell: Ni-YSZ|YSZ|YSZ-LSM|LSM. After sintering, the electrolyte and YSZ-LSM electrode were 9 and 20 μm thick, respectively. The performances of these reactors were determined as fuel cells, operating with dry H_2, and as electrolysers, operating with CO/CO_2 in the ratio 1/9. At 788 °C, the peak fuel cell power density was 0.69 W cm^{-2}, and at a cell potential difference of 1.5 V, the electrolysis current density was 3.3 A cm^{-2}, indicating that the performance of inkjet-printed YSZ-LSM electrodes can exceed those fabricated by conventional powder mixing processes.

1. Introduction

Reversible solid oxide electrochemical reactors (SOERs) are attractive devices for grid-scale energy storage due to their high energy conversion efficiencies (85–90%) [1], fuel flexibility, non-requirement for precious metal catalysts, and decreased specific electrical energy requirement due to high-temperature operation (550–850 °C) [2]. Furthermore, when operating with CO, CO_2, and CH_4, they may be cost-competitive with pumped hydroelectric storage [3]. Over the last decade, much of the increase in performance of SOERs has been due to optimisation of the fabrication process and materials [4].

Inkjet printing is a low-cost, rapid, and a non-destructive manufacturing technology [5] that has been deployed to produce a variety of devices including electronic circuit components, solar cells, and sensors [6]. A key characteristic of inkjet printing is that material waste during production is comparatively low [6], and that the deposited layers can be as thin as *ca.* 1 μm, enabling a high degree of control over the thickness of printed films. Therefore, inkjet printing is well suited to the fabrication of the functional layers of SOERs.

In Part I [7] of this series, we demonstrated that inkjet-printed yttria-stabilised zirconia ($(Y_2O_3)_{0.08}(ZrO_2)_{0.92}$, YSZ) electrolytes for the cell Ni-YSZ|YSZ|YSZ-$La_{0.8}Sr_{0.2}MnO_3$ (LSM)|LSM, resulted in solid oxide electrolysers with performance comparable to that of conventionally-fabricated reactors operating with CO/CO_2 gas mixtures. However, the electrolyte was thick (23 μm) compared with other inkjet-printed YSZ electrolytes [8–11], so offering potential for performance enhancement, especially at lower temperatures. Furthermore, printing additional functional layers, *i.e.* the electrodes, can maximise utilisation of materials, minimising waste during fabrication, and increasing consistency of electrochemical performance between cells due to the high reproducibility of inkjet printing and long-term ink homogeneity.

Hitherto, a single study on the electrochemical performance of an inkjet-printed YSZ-LSM composite O_2 electrode has been reported [12]. The cell performance was limited by dense film formation at the outer surface of the electrode ('skin'), which decreased the rates of diffusion of O_2 to active triple phase boundaries (TPBs). If this cell was adapted to operate in electrolysis mode, the dense film could become particularly problematic by preventing O_2 gas evolved at the anode from escaping, resulting in an increase in O_2 partial pressure within the electrode, diminishing kinetics and possibly causing catastrophic failure throughout the electrode over operational times required for seasonal energy storage [13].

Herein, we report the formulation of a composite YSZ-LSM ink and the fabrication and electrochemical characterisation of: Ni-

* Corresponding author.
E-mail address: g.kelsall@imperial.ac.uk (G.H. Kelsall).

https://doi.org/10.1016/j.electacta.2018.03.095

YSZ|YSZ(printed)|YSZ-LSM(printed)|LSM, in which the YSZ-LSM electrode does not have a dense outer skin. The objective was to determine whether or not, by optimising the ink formulation, solid oxide electrochemical reactors fabricated by inkjet printing could achieve performances, in H_2 fuel cell mode and when fed with CO/CO_2 in electrolyser mode, which exceed those produced by conventional powder mixing.

2. Materials and methods

Yttria-stabilised zirconia ($(Y_2O_3)_{0.08}(ZrO_2)_{0.92}$, YSZ, Sigma Aldrich, USA) and lanthanum strontium manganite ($La_{0.8}Sr_{0.2}MnO_3$, LSM, Fuel Cell Materials, USA) were dispersed using an ultrasonication probe (Q55, 20 kHz, 6 mm Ti alloy tip, QSonica, USA) by 3 × 3 min bursts, with a 3 min cooling interval. Particle size and zeta-potential were measured by dynamic light scattering and electrophoresis, respectively, using a Zetasizer mV instrument (Malvern, UK) with aqueous-based dispersions. Mass-specific surface area, was measured by BET using a Micrometrics 3Flex machine (Canada), respectively. Centrifugation (Eppendorf 5810 R, Germany) was used to narrow the particle size distributions in the dispersions by removing large aggregates. Viscosity and surface tension of the final formulations were measured with a DV-E Viscometer (Brookhaven, USA) and tensiometer (Model 250-U1, Ramé-hart, USA), respectively. Thermogravimetric analysis (TGA) was conducted using a Netzsch TG 209F1 Libra (USA), temperature ramp rate 4 °C min^{-1} in air with a 50 cm^3 min^{-1} flow rate.

YSZ specific surface area and particle size distribution (PSD) of the same particle source have been reported previously [7]. The dispersant used for the YSZ particles in water was Dispex A40 (BASF, Germany). The specific surface area and mean particle size of the LSM particles were measured respectively as 6.32 m^2 g^{-1} and 230 nm, as shown in Fig. S1. The polydispersity index (PDI) and particle size standard deviation of the LSM particles were 0.226 and 46 nm, respectively.

2.1. Aqueous YSZ ink formulation

It is preferable to fabricate cells with thin electrolytes, to decrease ohmic potential losses, but also to maintain ≥ 4 printed layers (1 in each of the 'positive' and 'negative' x and y printing directions) to ensure that defects resulting from missed droplet ejections may be covered by droplets in subsequently printed layers. Therefore, the YSZ ink was formulated as reported previously [7], but its mass fraction was decreased to 19 wt%. The zeta potential variation of the YSZ particles with Dispex A40 concentration (10^{-2} M KCl) is shown in Fig. 1. At the optimum concentration of 0.2 mg m^{-2}, the zeta potential was *ca.* −47 mV. Therefore, for the composite YSZ-LSM aqueous-based ink, it was necessary to negatively charge the LSM particles to prevent heterocoagulation.

2.2. Aqueous LSM ink formulation

As stability to aggregation for particulate dispersions of a metal oxide depends on pH, adsorbate concentration and ionic strength [14], the effects were investigated of varying pH (with nitric acid and ammonium hydroxide for acidic and basic conditions, respectively) and concentrations of a variety of dispersants on the zeta potential/surface charge of dispersed LSM particles in de-ionized water with 10^{-2} M KCl.

Fig. 2 shows the effect of pH on zeta potentials of LSM particles dispersed in aqueous 10^{-2} M KCl, suggesting an isoelectric point of *ca.* pH 3–6, poorly defined because of dissolution and colloidal instability at low zeta potentials, causing particle aggregation and sedimentation during measurements. Similar results were reported

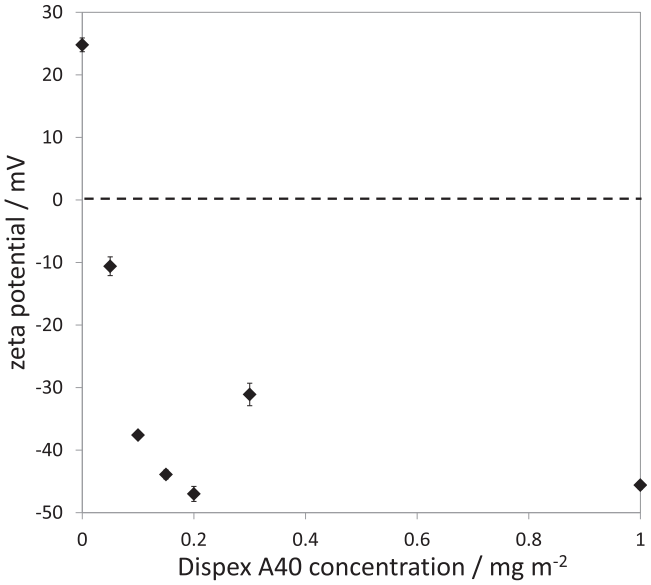

Fig. 1. Effect of Dispex A40 concentration on zeta potentials of YSZ particles in 10^{-2} M aqueous KCl.

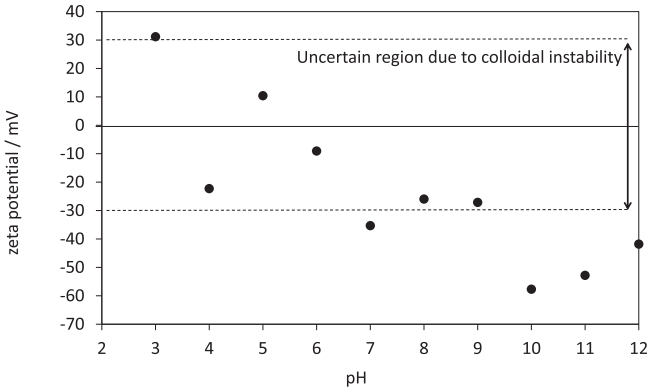

Fig. 2. Effect of pH on zeta potential of LSM particles dispersed in aqueous 10^{-2} M KCl.

previously [15], but significant dissolution of all components was measured at pH < 7, confirming LSM's instability under such conditions.

As the zeta potential of the Dispex-stabilised YSZ was negative (Fig. 1), greater values of pH were predicted to produce negatively-charged surfaces on both YSZ and LSM particles, thereby preventing their mutual hetero-coagulation within composite LSM-YSZ dispersions. Whereas Fig. 2 shows the maximum magnitude of zeta potential, and so predicted colloid stability, was achieved at pH 10 for LSM, that condition led to rapid aggregation and sedimentation at practical solid concentrations for an ink (> 5 wt%). Hence, to further increase particle surface charge and to inhibit dissolution processes, electrostatic dispersants listed in Table 1 were trialled to stabilise LSM dispersions against aggregation. According to electrophoretic mobility measurements, aluminon (tri-ammonium aurintricarboxylate; chemical structure shown in Fig. 3) was the only dispersant listed in Table 1 to adsorb on LSM, decreasing particle sedimentation rates; the other dispersants had no effect on particle colloidal stability. Lanthanum(III) and manganese(III,IV) are known to form carboxylates, providing a mechanism by which aluminon may adsorb on LSM particles.

Fig. 3 shows the effect of aluminon concentration on zeta potential of LSM particles dispersed in water at pH 10, exhibiting a